Flexural Strength Assessment of Ferrocement Confined Reinforced Concrete (FCRC) Beams

Seshu, D.R*

The characteristic equation of the stress strain curve for ferrocement confined reinforced concrete (FCRC) is used to evolve a procedure for generating the complete moment – curvature diagrams of FCRC sections. The validity of the procedure has been verified by an experimental investigation on 30 reinforced concrete beams confined with ferrocement in addition to stirrups at critical section. The correlation between the experimental and analytical values of ultimate moments and corresponding curvatures, arrived at, based on the above procedure is found to be good.

LIST OF SYMBOLS

D,b	=	Lateral dimensions of beam	M'_{ue}	=	$M_{ue}/f_{ck}\,b\,d^2$
d	=	Effective depth	M'_{ut}	=	$M_{ut}/f_{ck}\,b\,d^2$
f, ε	=	Stress and Corresponding strain	C_i	=	Confinement Index [Ref.9]
C_f	=	Compression force in FCRC	M_c	=	Moment of C_f about neutral axis
f_{cf}	=	Ultimate strength of FCRC	ε_{cf}	=	Strain at ultimate of FCRC
f_{ck}	=	Concrete cube strength	ϕ_{ue}	=	Experimental curvature at Ult.
A_b	=	Gross cross sectional area of ferrocement	ϕ_{ut}	=	Theoretical curvature at Ult.
V_f	=	Volume fraction	ϕ'_{ue}	=	$\phi_{ue} \times d$
f_{fs}	=	Stress in ferrocement shell	ϕ'_{ut}	=	$\phi_{ut} \times d$
η	=	Efficiency factor of the mesh	M_{ue}	=	Experimental Ultimate moment
S_f	=	Specific Surface Factor [Ref: 10]	M_{ut}	=	Theoretical Ultimate moment

INTRODUCTION

The problem of ensuring adequate ductility of concrete structures has been engaging the attention of several researchers nowadays. Ductility [1] is necessary for any structure to (i) give sufficient warning before failure, (ii) absorb strain energy due to dynamic forces (iii) allow full redistribution of moments in indeterminate structures, (iv) simplify the analysis of indeterminate structures and (v) accommodate any stresses due to accidental overloads, foundation settlements and volume changes. At present it is known that the ductility of concrete can be improved by confining the concrete in steel binders and such concrete being called as confined concrete or ductile concrete [2,3]. The spacing limitations on stirrups, limit the confinement offered by the stirrups [3,4]. To overcome this, the confinement due to ferrocement has been suggested as one of the alternatives [6-9]. Such concrete confined with ferrocement was termed as Ferrocement Confined Reinforced Concrete (FCRC)[10, 11]. Further, the investigation on FCRC revealed that the additional confinement with

* Assistant Professor, Department of Civil Engineering, Regional Engineering College, Warangal – 506 004, Andhra Pradesh, India. E-mail: drseshu@recw.ernet.in

ferrocement, improved the ultimate strength and strain of concrete [7, 10, 12]. The expressions for estimating the improvement in strength and strain of FCRC and the characteristic equation for stress-strain curve of FCRC have also been proposed [13, 14]. This paper presents a theoretical procedure, based on characteristic stress-strain curve of FCRC, for the assessment of moments and curvatures of FCRC sections. The method proposed has been validated by conducting experimental investigation on 30 reinforced concrete simply supported beams confined with ferrocement at critical sections.

STRESS-STRAIN CURVE OF FCRC

The stress – strain curve of FCRC as proposed by the author [14] is of the form:

$$f = [A\varepsilon/(1 + B\varepsilon + C\varepsilon^2)] \qquad \text{.....(1)}$$

The shape of the stress-strain diagram is shown in Fig. 1. The constants A, B and C that satisfy the boundary conditions are:

$$A = A'(f_{cf}/\varepsilon_{cf}) \qquad B = B'(1/\varepsilon_{cf}) \qquad C = C'(1/\varepsilon_{cf}^2)$$

where, $A' = 8.739$; $B' = 6.739$; $C' = 1.0$ for Ascending Portion
$A' = 4.286$; $B' = 2.286$; $C' = 1.0$ for Descending Portion of the stress-strain curve

$$f_{cf} = f_c'(1 + 0.55\,C_f)\,(0.9 + 0.055\,S_f) \qquad \text{.....(2)}$$

$$\varepsilon_{cf} = \varepsilon_c'(1 + 5.2\,C_f)\,(0.9 + 0.178\,S_f) \qquad \text{.....(3)}$$

The strain at 0.85 times ultimate stress is:

$$\varepsilon_{0.85cf} = \varepsilon_{cf}(2.237 + 0.1028\,S_f) \qquad \text{.....(4)}$$

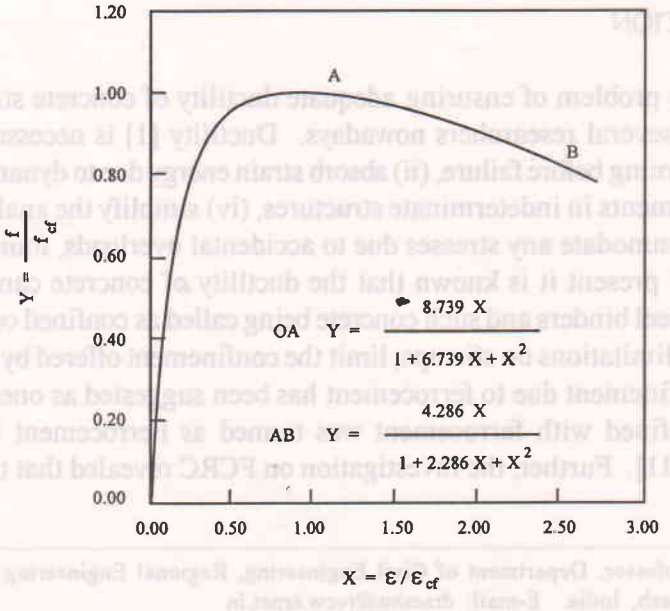

Fig. 1. Characteristic stress ratio (Ref. 14) vs. strain ratio ($\varepsilon/\varepsilon_{cf}$).

essions for
ı for stress-
procedure,
rvatures of
vestigation
ections.

.....(1)

and C that

ırve

.....(2)

.....(3)

.....(4)

DEVELOPMENT OF MOMENT-CURVATURE DIAGRAMS FOR FCRC SECTIONS

It becomes necessary to compute the total compressive force developed in a FCRC cross section and the moment of compressive force about the neutral axis for any extreme fiber concrete strain, in order to generate the moment–curvature diagram of any cross section. It can be seen that for any concrete strain (ε_c), in the extreme fiber (Fig. 2)

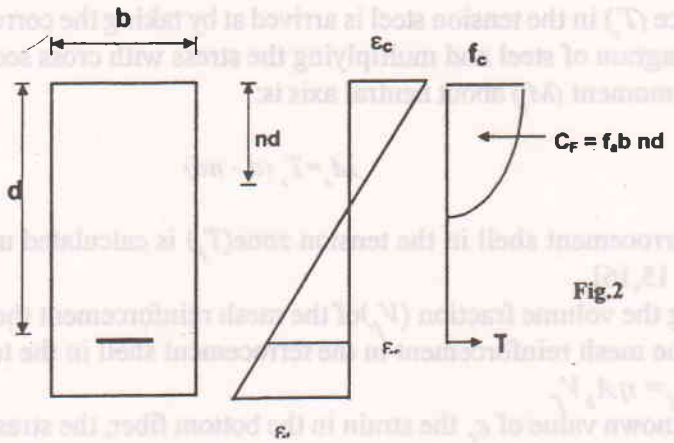

Fig.2

Fig. 2. Compressive forces and moment of compressive forces in FCRC.

$$C_F = f_a b\, n\, d \qquad .....(5)$$

where, $f_a = (1/\varepsilon_c)\int_0^{\varepsilon_c} f\,d\varepsilon$

$$M_c = b\,(nd/\varepsilon_c)^2 \int_0^{\varepsilon_c} f\varepsilon\,d\varepsilon \qquad .....(6)$$

The corresponding curvature can be obtained by : $\phi_c = (\varepsilon_c/nd)$

The evaluation of intergrals $\int_0^{\varepsilon_c} f\,d\varepsilon$ and $\int_0^{\varepsilon_c} f\varepsilon\,d\varepsilon$ leads to the expressions:

$$C_f = bnd/\varepsilon_c (AK_1/2C - ABK_2/2C^2) \qquad .....(7)$$

$$M_c = (nd/\varepsilon_c)^2 b\,\{A\varepsilon_c/C - ABK_1/2C^2 + A/2C^3\,(B^2 - 2C)\,K_2\} \qquad .....(8)$$

where $K_1 = \ln(1 + B\varepsilon_c + C\varepsilon_o^2)$.

K_2 will have three expressions depending on $4C - B^2$, as follows:

For $4C - B^2 < 0.0$ and $Q = \sqrt{B^2 - 4C}$ $\quad K_2 = C/Q \ln\{(2C\varepsilon_c + B - Q)(B + Q)/(2C\varepsilon_c + B + Q)(B - Q)\}$

For $4C - B^2 = 0.0$; $\quad K_2 = 2A\varepsilon_c/(2C\varepsilon_c + B)$

For $4C - B^2 > 0.0$ and $R = \sqrt{4C - B^2}$ $\quad K_2 = (2C/R)\,\mathrm{Tan}^{-1}\{R\,\varepsilon_c/(2 + B\varepsilon_c)\}$

For obtaining the complete moment curvature relationship for any cross-section discrete values of extreme fiber concrete strains (ε_c) were selected such that even distribution of points on the plot, both

before and after the maximum moment, were obtained. The procedure used in computation is as follows:

1. For the selected value of ε_c, the extreme fiber concrete strain, the neutral axis depth, '*nd*' is assumed initially at a value of 0.5*d*.
2. For the assumed value of '*nd*', the compressive force (C_F) and the value of Moment (M_c) of this resultant compressive force about the neutral axis is calculated.
3. The strain in tension steel (ε_s) is calculated based on strain compatibility.
4. The tensile force (T_s) in the tension steel is arrived at by taking the corresponding stress from the stress-strain diagram of steel and multiplying the stress with cross sectional area of steel. The corresponding moment (M_s) about neutral axis is:

$$M_s = T_s (d - nd) \qquad \text{.....(9)}$$

5. The force in ferrocement shell in the tension zone(T_f) is calculated using the methodology as detailed below[15,16].
   i. Knowing the volume fraction (V_f)of the mesh reinforcement the effective cross sectional area of the mesh reinforcement in the ferrocement shell in the tension zone is calculated using $A_{cf} = \eta A_b V_f$
   ii. For the known value of ε_t the strain in the bottom fiber, the stress f_{fs} in the ferrocement is obtained using corresponding stress-strain diagram of the mesh steel. The stress when multiplied with effective cross sectional area of the ferrocement gives the force in the Ferrocement (T_f) in the tension zone and moment of this force about the neutral axis is obtained.
   iii. The total tensile force is arrived by $T = T_s + T_f$
6. The value of C_F and T are now compared. If C_F and T are same, then the assumed position of neutral axis is correct. Then the moment (M) and the curvature (ϕ) for that particular fiber strain in concrete are calculated as $M = M_c + M_s + M_f$ and $\phi_c = \varepsilon_c / nd$.
7. If C_F and T are not equal, a new value of the neutral axis depth is assumed based on judgment, whether C_F is greater or smaller than T, and the above procedure is repeated until the equilibrium condition $C_F = T$ is satisfied.

The above analytical procedure enables the assessment of flexural strength of FCRC sections. The assumptions made in deriving the flexural response are: (i) tensile strength of core concrete is neglected, (ii) mortar contribution towards the strength of ferrocement in tension is neglected, and (iii) variation of strain across the section is linear up to failure.

In addition to the above assumptions, the three basic relationships viz., (i) equilibrium of forces, (ii) compatibility of strains, and (iii) stress–strain relationships of the material have to be satisfied.

PRESENT WORK

Results derived from the above-proposed analytical procedure are compared with the experimental data documented by the author [10, 15]. Details of comparison are shown in Table 1. The experimental programme included casting and testing of 30 reinforced concrete beams of size 120 mm x 200 mm x 2200 mm confined with ferrocement in addition to stirrups at critical zone, i.e. the zone in which the plastic hinge forms under flexure. The length of critical zone was arrived based on plastic hinge length criteria for confined concrete. All the beams were tested under symmetrical two – point loading on a simply supported span of 1700 mm. Specially fabricated curvature meters were used to

measure the curvatures in the central zone of 600 mm of the beam, in three gage lengths of 200 mm each. Strain rate control was used to obtain the complete profile of moment – curvature behavior, especially in the post ultimate region. Moment – curvature diagrams generated for various cross sections based on the stress – strain diagrams for FCRC are shown by firm lines in Fig. 3. The experimental values of moments and curvatures are plotted as discrete points on the above moment – curvature diagrams. The experimental ultimate moments and theoretical moments computed based on stress-strain of FCRC are represented on a correlation diagram shown in Fig. 4.

CORRELATION

It can be seen from Fig. 3, that the procedures developed for obtaining the complete profile of moment – curvature diagram of FCRC sections, based on the stress-strain curves of FCRC predict the experimental behavior satisfactorily. There is a fairly good agreement between the analytical and experimental ultimate moments, as can be seen from the correlation diagram shown in Fig. 4. The average ratio of the experimental to analytical ultimate moments is 1.024 with a standard deviation of 0.0386 and co-efficient of variation of 3.78%. The correlation between experimental and analytical ultimate curvatures is not so good as that of ultimate moments. A limit of steel strain of 4% is imposed on analytical ultimate curvatures, corresponding to the minimum failure strain of tor steel specimens observed in the tests. The average ratio of the experimental to analytical curvature is 0.756, with a standard deviation of 0.243, and a co-efficient of variation of 32.09%. The lack of very good correlation in curvatures may be attributed to the fact that the analytical curvature is the curvature at a section, computed to satisfy the equilibrium and compatibility conditions and material properties. The experimental curvature is the curvature measured over a gage length of 200 mm and hence represents the average curvature over a gage length, including localized high curvatures at cracks. Hence, the average curvature depends upon the number of cracks occurring in the gage length, their width, distribution and location. The occurrence and location of cracks once again depends upon a number of factors, prominent among them being, uniformity of strength of concrete in the critical zone and local variation of bond between steel and concrete. The provision of ferrocement transforms the brittle behavior of over reinforced RC sections into ductile ones (Fig.3) by developing moment curvature diagrams with more horizontal plateau in post ultimate regions.

IDEALIZATION OF MOMENT-CURVATURE DIAGRAM

A critical appraisal of the moment – curvature diagrams of FCRC beams, shows that the moment – curvature diagrams can be idealized as a bilinear form consisting of two straight lines, one inclined raising straight line up to 90% of the ultimate moment of that FCRC beam and other line is a horizontal straight line at the end of the raising straight line. This idealization leads to the assumption that up to 90% of the ultimate moment, the FCRC cross-section behaves elastically and beyond this value, the behavior is completely plastic. The assumption of elastic behavior up to such a high value of ultimate moment seems to be justified for reinforced concrete section confined additionally with ferrocement shell, though not an ordinary RC section. The slope of the raising line in the idealized diagram is equal to the flexural rigidity 'EI' of the cross section. The value of 'I', the moment of inertia of the cross section is calculated based on uncracked transformed cross-section, taking the steel area also into consideration. The value of 'E' is the initial modulus of elasticity of concrete and can be calculated from the formula $E = 17500\sqrt{f_c'}$. The limit for the horizontal straight line may be taken as that point where this idealized straight line cuts the actual moment-curvature diagram. If due to the

Table 1 Comparison of Experimental with Theoritical Values, Ultimate Moments and Curvature of FCRC Beams

Sl. No.	Desig. Of Beam	S_f	Experimental		Theoretical		M'_{ue}/M'_{ut}	ϕ'_{ue}/ϕ'_{ut}
			M'_{ue}	$\phi'_{ue} \times 10^{-4}$	M'_{ut}	$\phi'_{ut} \times 10^{-4}$		
1	2	3	4	5	6	7	8	9
1	AUM0	0.000	0.2471	23.87	0.2422	39.54	1.020	0.603
2	AUM1	1.649	0.2522	25.50	0.2461	44.60	1.024	0.572
3	AUM2	3.298	0.2568	33.25	0.2524	63.60	1.017	0.522
4	AUM3	4.947	0.2595	45.47	0.2580	97.75	1.000	0.465
5	AUM4	6.597	0.2618	61.30	0.2633	98.61	0.994	0.621
6	ABM0	0.000	0.3394	18.70	0.3213	36.45	1.056	0.513
7	ABM1	1.576	0.3456	25.92	0.3346	38.67	1.032	0.670
8	ABM2	3.152	0.3681	30.33	0.3447	55.60	1.067	0.545
9	ABM3	4.728	0.3730	33.32	0.3548	82.12	1.051	0.405
10	ABM4	6.304	0.3790	50.48	0.3637	112.52	1.042	0.448
11	AOM0	0.000	0.4018	16.11	0.4236	15.66	0.948	1.028
12	AOM1	1.653	0.4122	20.26	0.4279	20.77	0.963	0.975
13	AOM2	3.307	0.4427	27.64	0.4467	27.21	0.991	1.015
14	AOM3	4.960	0.4231	34.93	0.4652	36.92	0.909	0.946
15	AOM4	6.614	0.4776	40.80	0.4834	49.42	0.988	0.825
16	BUM0	0.000	0.2444	24.35	0.2419	45.27	1.010	0.538
17	BUM1	1.637	0.2515	33.49	0.2443	50.62	1.029	0.661
18	BUM2	3.295	0.2576	48.12	0.2494	78.20	1.032	0.615
19	BUM3	4.912	0.2602	50.45	0.2510	105.15	1.036	0.479
20	BUM4	6.550	0.2610	44.45	0.2563	103.49	1.018	0.429
21	BBM0	0.000	0.3259	19.24	0.3021	21.77	1.078	0.884
22	BBM1	1.621	0.3554	23.74	0.3233	30.06	1.099	0.789
23	BBM2	3.242	0.3488	41.46	0.3330	42.42	1.047	0.977
24	BBM3	4.863	0.3595	45.80	0.3425	58.87	1.049	0.777
25	BBM4	6.484	0.3659	51.70	0.3518	82.84	1.040	0.978
26	BOM0	0.000	0.4101	15.41	0.3973	15.48	1.032	0.995
27	BOM1	1.577	0.4082	20.50	0.4027	19.25	1.013	1.064
28	BOM2	3.154	0.4332	29.24	0.4214	24.51	1.028	1.192
29	BOM3	4.731	0.4665	37.53	0.4378	33.72	1.065	1.113
30	BOM4	6.309	0.4755	46.52	0.4542	43.97	1.046	1.057
Average							1.024	0.7567
Standard Deviation							0.0386	0.2428
Co-efficient of Variation							3.778	32.091

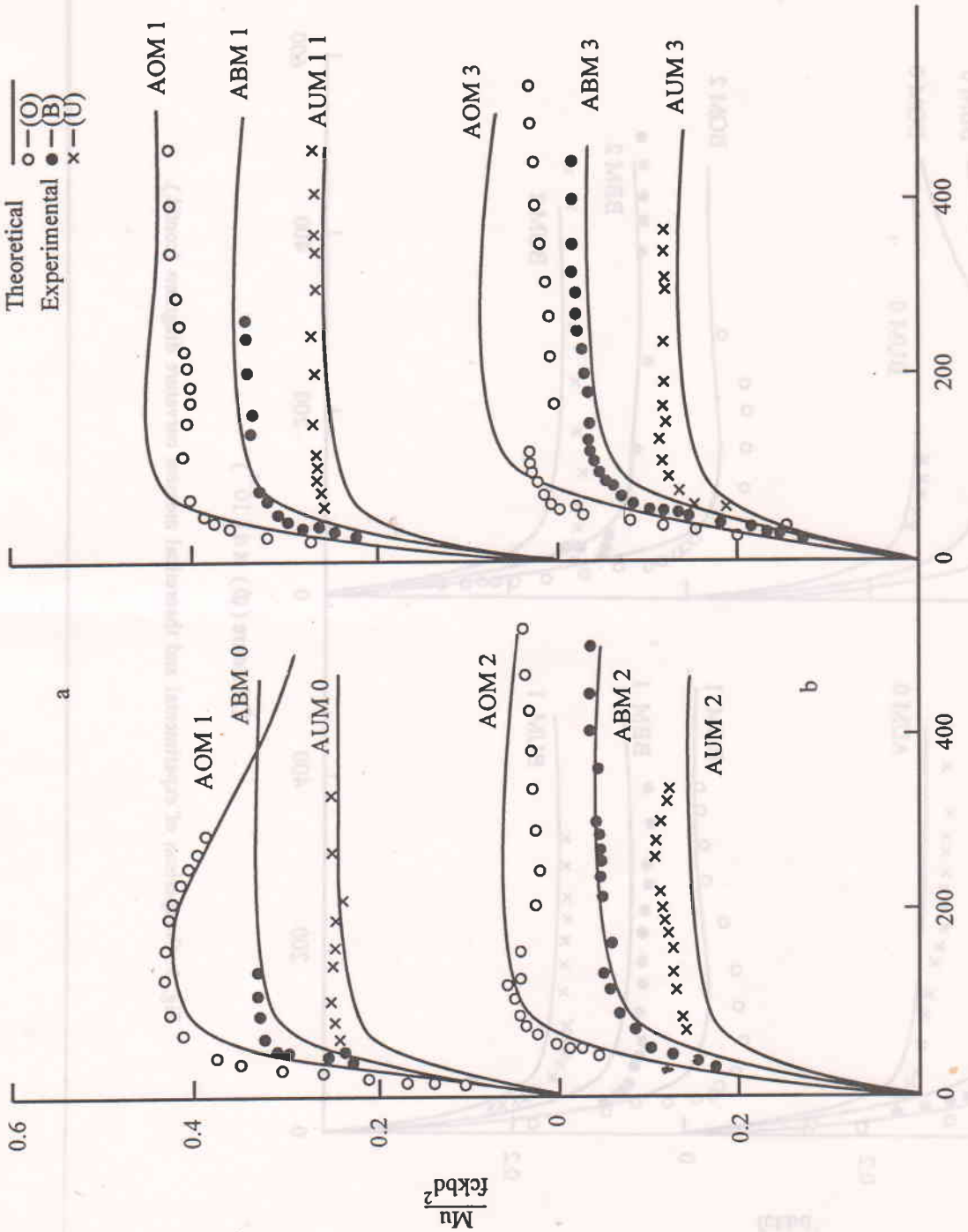

Fig. 3. Comparison of experimental and theoretical moment curvature diagrams.

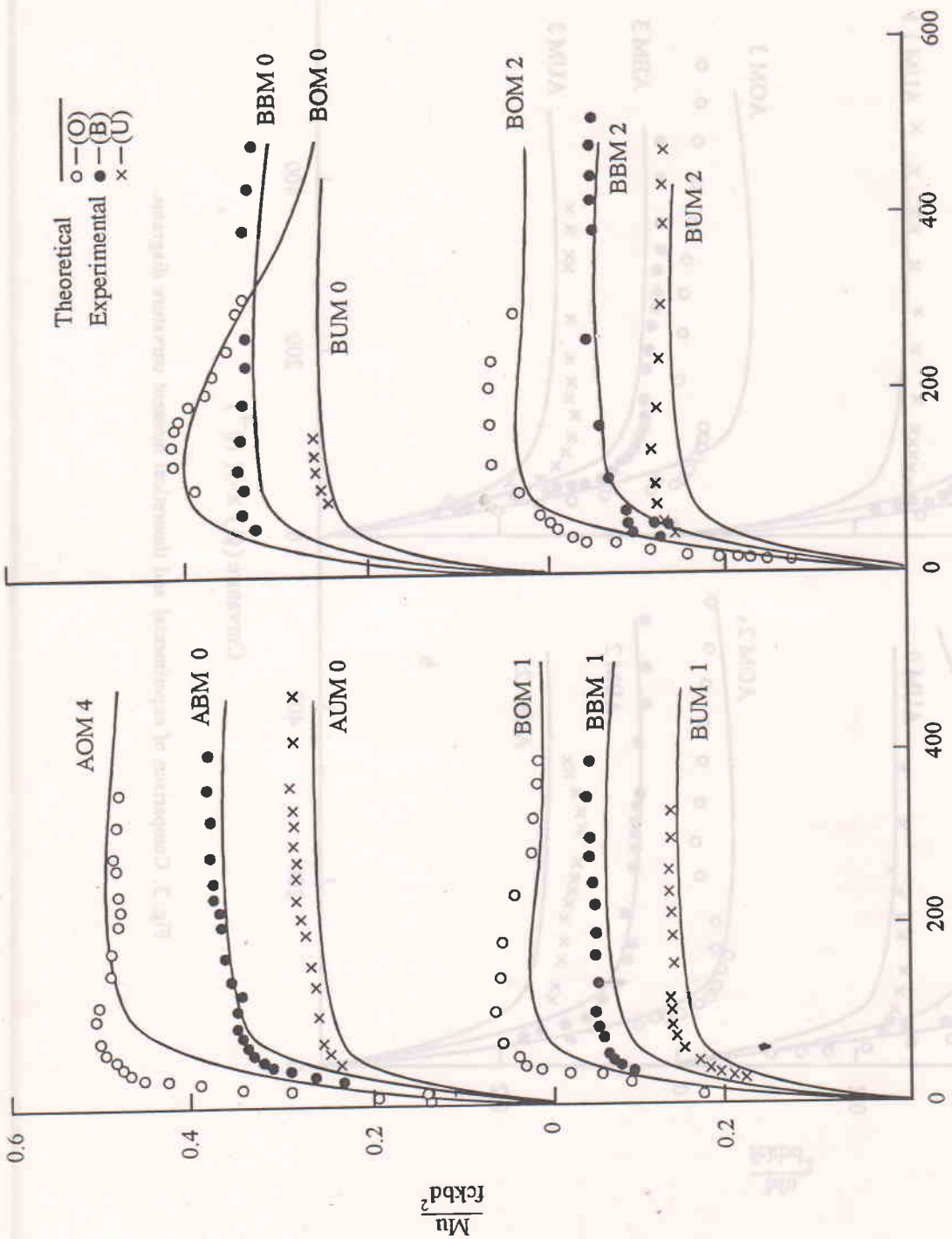

Fig. 3. Comparison of experimental and theoretical moment curvature diagrams (cont'd.).

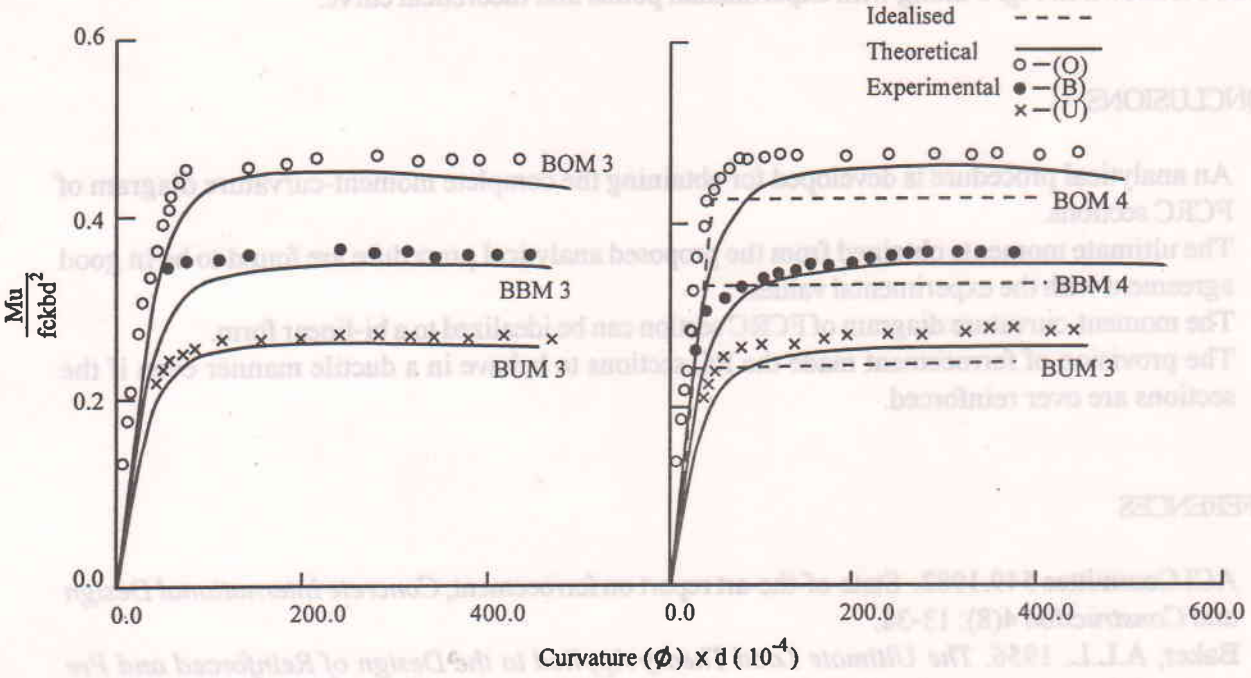

Fig. 3. Comparison of experimental and theoretical moment curvature diagrams (cont'd.).

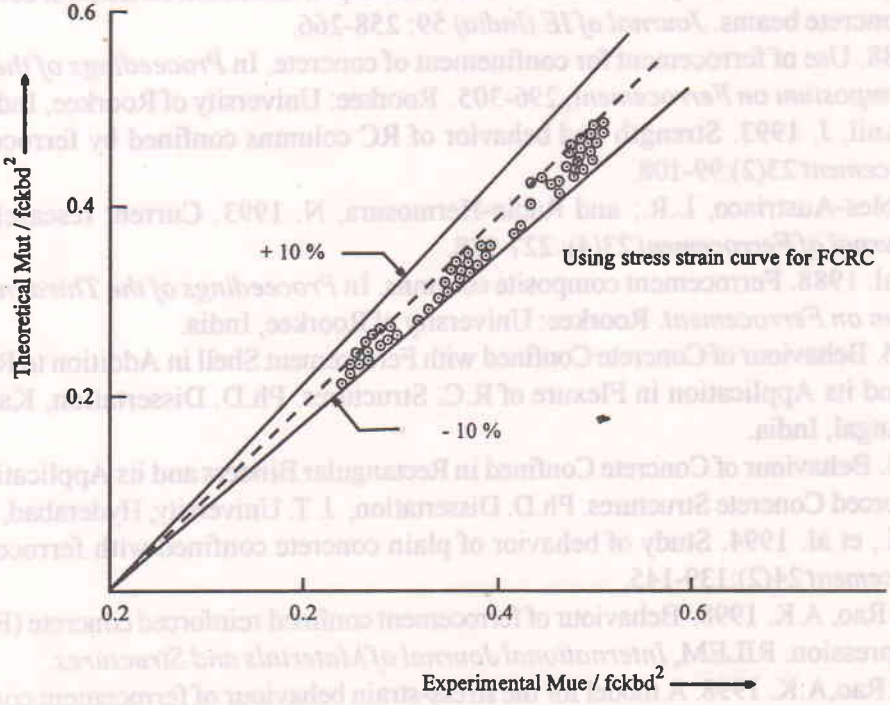

Fig. 4. Correlation diagram for ultimate moments.

hyper resistance of tor-steel above 0.2% proof stress, for higher confinement indices and specific surface factor values, the horizontal straight line may not cut the actual moment-curvature diagram, in which the strain limits can be imposed. A typical idealized moment-curvature diagram for FCRC section is shown in Fig. 3 along with experimental points and theoretical curve.

CONCLUSIONS

1. An analytical procedure is developed for obtaining the complete moment-curvature diagram of FCRC sections.
2. The ultimate moments obtained from the proposed analytical procedure are found to be in good agreement with the experimental values.
3. The moment-curvature diagram of FCRC section can be idealized to a bi-linear form.
4. The provision of ferrocement made the RC sections to behave in a ductile manner even if the sections are over reinforced.

REFERENCES

1. ACI Committee 549.1982. State-of-the-art report on ferrocement, *Concrete International Design and Construction* 4(8): 13-38.
2. Baker, A.L.L. 1956. *The Ultimate Load Theory Applied to the Design of Reinforced and Pre stressed Cncrete Fames*. London: Concrete Publications Ltd.
3. Sheikh, S.A.1982. Comparative study of confinement models. *ACI Journal* 79 (4): 296-306.
4. Paulay and Priestley, M.J.N.. 1992. *Seismic Design of Reinforced Concrete and Masonry Buildings*. New York: John Wiley and Sons.
5 Rao, A.K.; Reddy, K.N.; and Reddy, V.M. 1979. Effect of stirrup confinement on flexural behaviour of prestressed concrete beams. *Journal of IE (India)* 59: 258-266.
6. Balaguru, P. 1988. Use of ferrocement for confinement of concrete. In *Proceedings of the Third International Symposium on Ferrocement*, 296-305. Roorkee: University of Roorkee, India.
7. Ganesan, and Anil, J. 1993. Strength and behavior of RC columns confined by ferrocement. *Journal of Ferrocement* 23(2):99-108.
8. Pama, R.P.; Robles-Austriaco, L.R.; and Rubio-Hermosura, N. 1993. Current researches on ferrocement. *Journal of Ferrocement* 23(4): 227-288.
9. Singh, K.K., et al. 1988. Ferrocement composite columns. In *Proceedings of the Third International Symposium on Ferrocement.* Roorkee: University of Roorkee, India.
10. Seshu, D.R. 1995. Behaviour of Concrete Confined with Ferrocement Shell in Addition to Rectangular Stirrups and its Application in Flexure of R.C. Structures. Ph.D. Dissertation, Kakatiya University, Warangal, India.
11. Reddy, S.R. 1974. Behaviour of Concrete Confined in Rectangular Binders and its Applications in Flexure of Reinforced Concrete Structures. Ph.D. Dissertation, J. T. University, Hyderabad, India.
12. Waliuddin, A.M., et al. 1994. Study of behavior of plain concrete confined with ferrocement. *Journal of Ferrocement* 24(2):139-145.
13. Seshu, D.R., and Rao, A.K. 1998. Behaviour of ferrocement confined reinforced concrete (FCRC) under axial compression. RILEM, *International Journal of Materials and Structures*.
14. Seshu, D.R., and Rao,A.K. 1998. A model for the stress-strain behaviour of ferrocement confined reinforced concrete (FCRC) under axial compression. *Journal of Ferrocement* 28(2): 147-164.
15. Seshu, D.R. 1999. Flexural behavior of ferrocement confined reinforced concrete (FCRC) simply supported beams. *Journal of Ferrocement* 30(3).

16. Huq, S., and Pama, R.P. 1978. **Ferrocement in flexure: Analysis and design.** *Journal of Ferrocement* 8(3): 169-193.
17. Mansur, M.A., and Paramasivam. 1986. **Cracking behavior and ultimate strength of ferrocement in flexure.** *Journal of Ferrocement* 16(4): 405 – 415.